Mineralogical Magazine (2024), **88**, 31–39
doi:10.1180/mgm.2023.78

CAMBRIDGE UNIVERSITY PRESS

Article

Okruginite, Cu_2SnSe_3, a new mineral from the Ozernovskoe deposit, Kamchatka peninsula, Russia

Anna Vymazalová[1], Vladimir V. Kozlov[2], František Laufek[1], Chris J. Stanley[3], Ilya A. Shkilev[4], Sharapat Kudaeva[5] and Filip Košek[6]

[1]Czech Geological Survey, Geologická 6, 152 00 Prague, Czech Republic; [2]IGEM RAS, 35, Staromonetny lane, Moscow, 119017, Russia; [3]Department of Earth Sciences, Natural History Museum, London SW7 5BD, UK; [4]JSC "Siberian Mining and Metallurgical Alliance", Mishennaya 106, Petropavlovsk-Kamchatsky, Kamchatka Territory, 683016, Russia; [5]Institute of Volcanology and Seismology, Russian Academy of Science, Petropavlovsk-Kamchatsky, 683006, Russia; and [6]Institute of Geochemistry, Mineralogy and Mineral Resources, Faculty of Science, Charles University, Albertov 6, 128 00 Prague, Czech Republic

Abstract

Okruginite, Cu_2SnSe_3 is a new mineral discovered from the high-sulfidation epithermal Au Ozernovskoye deposit, Kamchatka peninsula, Russia. It occurs as distinct Se-rich zones in Se-bearing mohite crystals or forms aggregates of small crystals 10–15 μm in size in quartz. In plane-polarised light, okruginite appears brownish grey. Pleochroism and bireflectance are discernible, anisotropy is weak, with rotation tints pale blue-grey to pale grey-brown; it exhibits no internal reflections. Reflectance values of the synthetic analogue of okruginite in air (R_1, R_2 in %) are: 25.9, 26.5 at 470 nm, 27.5, 26.5 at 546 nm, 27.8, 28.4 at 589 nm and 27.7, 28.4 at 650 nm. Twenty seven electron-microprobe analyses of okruginite give an average composition: Cu 29.48, Sn 28.10, Se 33.40 and S 8.75, total 99.73 wt.%, corresponding to the empirical formula $Cu_{1.99}Sn_{1.02}(Se_{1.82}S_{1.17})_{\Sigma 2.99}$ based on 6 atoms; the average of seven analyses on its synthetic analogue is: Cu 23.62, Sn 24.37 and Se 49.09, total 97.08 wt.%, corresponding to $Cu_{1.86}Sn_{1.03}Se_{3.11}$. The density, calculated on the basis of the empirical formula, is 5.126 g/cm^3. The mineral is monoclinic, space group *Cc*, with $a = 6.9906(2)$, $b = 12.0712(4)$ Å, $c = 6.9723(2)$ Å, $\beta = 109.350(10)°$, $V = 555.1(2)$ Å^3 and $Z = 4$. The crystal structure was solved and refined from the powder X-ray-diffraction data of synthetic Cu_2SnSe_3. Okruginite is the selenium-end member of the Cu_2SnS_3–Cu_2SnSe_3 solid solution. The mineral name is in honour of Dr. Victor Mikhailovich Okrugin, a Russian mineralogist, for his contributions to mineralogy and geology of epithermal deposits, in particular of the Au–Ag deposits in Kamchatka.

Keywords: okruginite; Cu_2SnSe_3; electron-microprobe data; reflectance data; X-ray-diffraction data; crystal structure; Ozernovskoe deposit; Kamchatka; Russia

(Received 15 April 2023; accepted 2 October 2023; Accepted Manuscript published online: 16 October 2023; Associate Editor: Koichi Momma)

Introduction

Okruginite, Cu_2SnSe_3, the proposed new mineral, was discovered in quartz veins of the Au–Te–Se volcanic-hosted high-sulfidation epithermal Au deposit Ozernovskoe, Kamchatka peninsula, Russia (57°35'36"N, 160°50'60"E). It occurs in bonanza Au–Te ores in an early paragenesis with quartz, cassiterite, rutile, and Sn-, W-, Mo-bearing sulfides and sulfoselenides (Se-herzenbergite, Se-mawsonite, Se-stannite and kiddcreekite) followed by later ore minerals (fahlerz, chalcopyrite, Bi and Bi–Pb selenotellurides, Au, Ag, Cu tellurides and native tellurium). The latest tellurides and native tellurium are deposited in a paragenesis with quartz and Mn-bearing dolomite. This paragenetic sequence possibly reflects a fluid boiling process: a rapid temperature drop from 300–350°C to 150–180°C and pH increase due to loss of H_2S and other volatiles to the gas phase. It leads to the formation of extremely rich and complex bonanza ores with banded and breccia textures.

Corresponding author: Anna Vymazalová; Email: anna.vymazalova@geology.cz
Cite this article: Vymazalová A., Kozlov V.V., Laufek F., Stanley C.J., Shkilev I.A., Kudaeva S. and Košek F. (2024) Okruginite, Cu_2SnSe_3, a new mineral from the Ozernovskoe deposit, Kamchatka peninsula, Russia. *Mineralogical Magazine* **88**, 31–39. https://doi.org/10.1180/mgm.2023.78

Both the mineral and name (symbol Okg) were approved by the Commission on New Minerals, Nomenclature and Classification of the International Mineralogical Association (IMA No 2022-096, Vymazalová *et al.*, 2022). The mineral is to honour Dr Victor Mikhailovich Okrugin (Виктор Михайлович Округин) (b. 1945, †2022), mineralogist from the Institute of Volcanology and Seismology, Far East Branch of Russian Academy of Sciences (IVS FEB RAS), for his contributions to mineralogy and geology of epithermal deposits, in particular of the Au–Ag deposits in Kamchatka. The material containing the proposed mineral was one of his last commenced research projects, he also discovered the mineral svetlanaite from the same type-sample (Okrugin *et al.*, 2022). The holotype material (polished section), along with its synthetic analogue (Exp Sn2), is deposited at the Department of Earth Sciences of the Natural History Museum, London, UK, catalogue number BM 2021, 02. The holotype material is also the type material for mineral svetlanaite (SnSe), IMA No 2020-013.

Okruginite is the selenium end-member of the Cu_2SnS_3–Cu_2SnSe_3 solid solution. According to the chemical composition, the mineral should belong to the 2.D (Metal Sulphides) category of the Nickel and Strunz classification (Strunz and Nickel (2001).

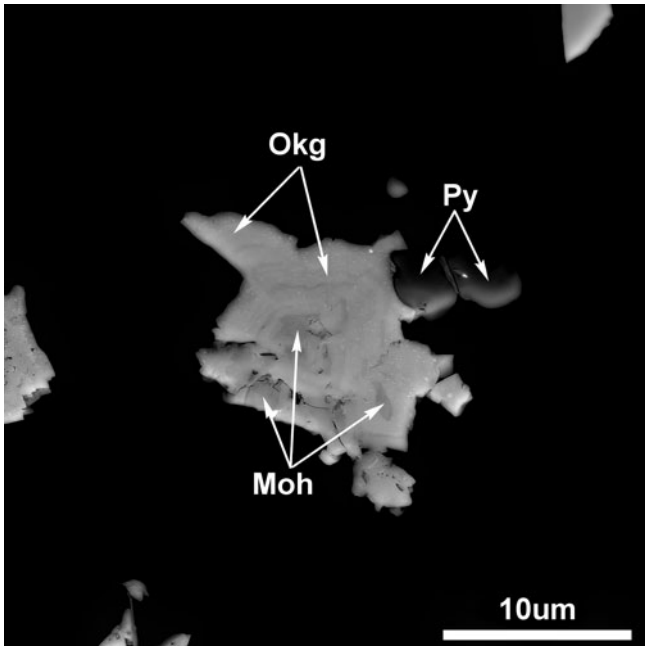

Figure 1. Okruginite (Okg) occurring as distinct Se-rich zones in Se-bearing mohite (Moh) crystal with pyrite (Py) in quartz (Qz). Back-scattered electrons image, holotype BM 2021, 02.

The most closely related mineral species is mohite Cu_2SnS_3, whose crystal structure has yet to be determined.

Geological setting, occurrence and associated minerals

The Ozernovskoe deposit is located within the North Kamchatka ore region of the Central Kamchatka volcanic belt, 140 km north of the town of Klyuchi and 80 km west of the Bering Sea coast (Okrugin *et al.*, 2022).

This Au–Te–Se deposit of epithermal high sulfidation type is localised within a Miocene basaltic palaeovolcano, composed of sills and dykes of andesite–basalts, cut by through by volcanic domes of andesites, andesite–dacites, dacites, magmatic breccias and tuffisites (Petrenko, 1999; Litvinov *et al.*, 1999; Demin, 2015). The ore-bearing quartz veins and stockworks are hosted by hydrothermal silification zones, consisting of quartz, kaolinite, dickite and alunite-group minerals.

This deposit is distinguished by a variety of selenide and telluride minerals, including some new and unnamed species (Kovalenker and Plotinskaya, 2005; Spiridonov *et al.*, 1990; 2009; 2014; Okrugin *et al.*, 2022) as well as the recently described minerals ozernovskite (Pekov *et al.*, 2021) and rudolfhermannite (Pekov *et al.*, 2022).

Ore deposition is related to multiple repeated cycles of extensive boiling and related hydrothermal brecciation. From one to five stages of ore minerals deposition can be recognised on every cycle. The earliest stage is represented by quartz + kaolinite + alunite-group minerals (woodhouseite, etc.) + anatase + rutile + zircon + pyrite followed by cassiterite with very rare scheelite, scandium-bearing titanite, and thortveitite. Cassiterite replaces rutile crystals epitaxially as revealed by electron back-scattering diffraction (EBSD) orientation mapping. Cassiterite from this locality is found to contain unusually high concentrations of W, Ga, V, Ti and Al substituting Sn. In rare cases it also contains Sc (up to 0.2–0.4 wt.%). Cassiterite–rutile crystals are usually overgrown and are partly replaced by Se-bearing mohite and okruginite with other Sn-, W-, Mo-bearing sulfides and sulfoselenides (Se-bearing herzenbergite and svetlanaite, Se-mawsonite, Se-stannite, kidd-creekite, hemusite) followed by other ore minerals (a variety of tetrahedrite-group minerals, chalcopyrite, Bi and Bi–Pb seleno-tellurides, Au, Ag, Cu tellurides, native tellurium and native Te–Se alloys). The latest tellurides and native tellurium were deposited in close paragenesis with quartz and Mn-bearing dolomite.

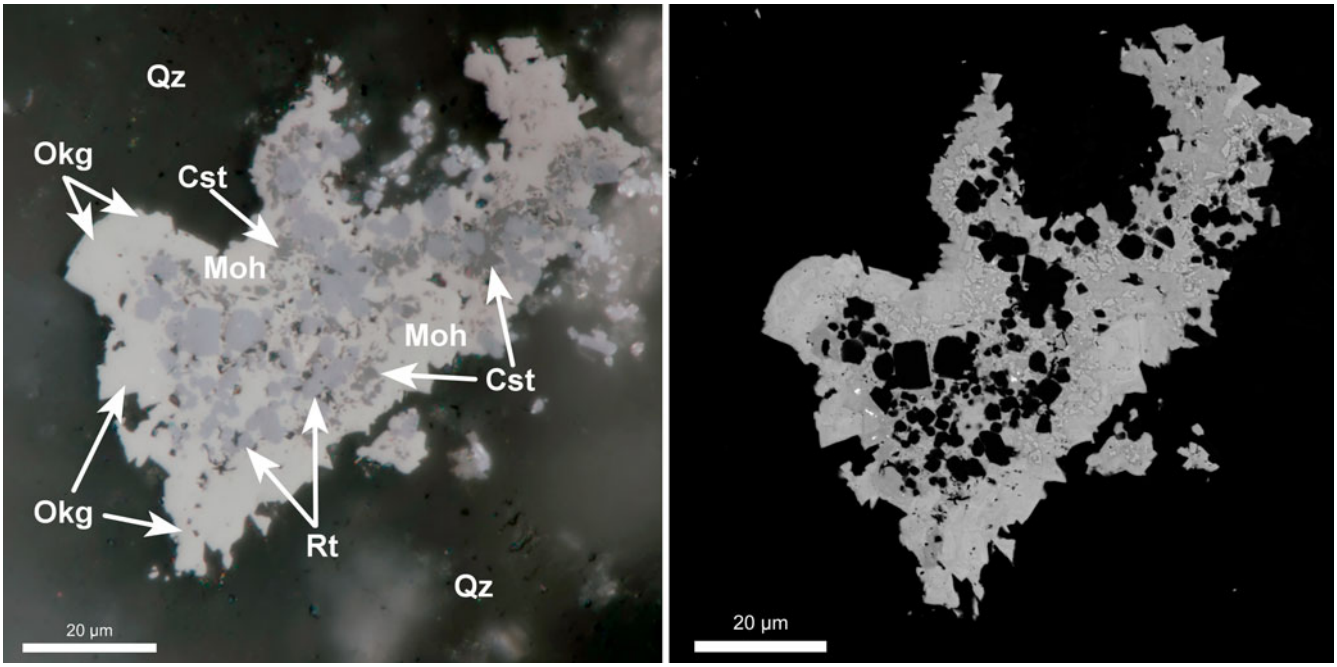

Figure 2. Reflected light (left) and back-scattered electrons (right) images of okruginite (Okg), brighter then mohite in BSE), Se-bearing mohite (Moh), cassiterite (Cst) and rutile (Rt) in quartz (Qz). Holotype BM 2021, 02.

https://doi.org/10.1180/mgm.2023.78 Published online by Cambridge University Press

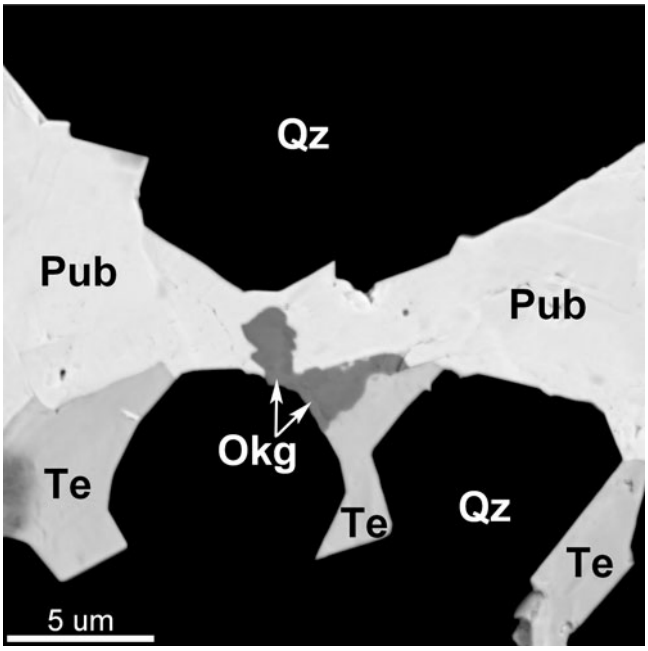

Figure 3. Back-scattered electrons image of okruginite (Okg) with poubaite (Pub) and native tellurium (Te) in quartz (Qz). Holotype BM 2021, 02.

Appearance, physical and optical properties

Okruginite occurs as distinct Se-rich zones in Se-bearing mohite crystals (Fig. 1) or forms aggregates of small crystals in size 10–15 μm in quartz and poubaite (Figs 2, 3). It occurs in association with cassiterite, rutile, mohite, mawsonite, kiddcreekite, hemusite, native tellurium, kostovite, Se-bearing fahlerz (Se-goldfieldite – Se (Bi)-tetrahedrite – Se-tennantite), svetlanaite and quartz.

Okruginite is opaque with a metallic lustre. The mineral is brittle. The density calculated on the basis of the empirical formula is 5.126 g/cm^3. In plane-polarised reflected light, okruginite appears brownish grey against rutile, cassiterite, chalcopyrite and other minerals in the natural assemblage. Okruginite has weak anisotropy with rotation tints pale blue-grey to pale grey-brown, bireflectance and pleochroism was not discernible. It exhibits no internal reflections.

Reflectance measurements were made in air relative to a WTiC standard using a J & M TIDAS diode array spectrometer attached to a Zeiss Axiotron microscope. The results in comparison with its synthetic analogue (Cu_2SnSe_3) are tabulated in (Table 1) and illustrated in Fig. 4.

Chemical composition

Chemical analyses were performed with a TESCAN LYRA3 FEG scanning electron microscope (SEM) with Shottky cathode located in the Kurchatov Institute, Moscow, Russia, using Oxford Instruments *Inca Wave and IncaEnergy*+ WDS–EDS system with Wave-500 WDS spectrometer and X-Max80 EDS detector. The following X-ray lines were used for quantification: Sn*Lα*, Se*Lα*, S*Kα*, Cu*Kα*, Fe*Kα*, Mn*Kα* and V*Kα*. The following conditions were applied for the data collection: wavelength dispersive spectroscopy; acceleration voltage of 20 kV; beam current of 12 nA, beam diameter of 1 μm, number of analyses = 27. Acquisition time was 30 s on peak and 15 × 2 s on background for major elements (Cu, Sn, Se and S) and 50 s on peak and 25 × 2 s on background for minor elements (V, Mn and Fe). The presence of Sb and Te was also tested for, but they were not detected. The MAC set of pure elements (for Sn, Se, Mn and V) and natural stoichiometric $CuFeS_2$ for Cu, Fe and S were used as standards. The matrix correction procedure of Pouchou and Pichoir (XPP), integrated in *Inca* software, was used.

Chemical analyses of the synthetic analogue were performed with a CAMECA SX-100 electron probe microanalyser in wavelength-dispersive mode using an electron beam focussed to 1–2 μm, located in the Institute of Geology, Academy of Sciences of the Czech Republic. Cuprite (Cu_2O) and pure Sn and Se were used as standards. Concentrations were quantified

Table 1. Reflectance data for okruginite and its synthetic analogue Cu_2SnSe_3.

	Okruginite						Synthetic Cu_2SnSe_3	
	Site 1		Site 2		Site 3			
λ (nm)	R_1 (%)	R_2 (%)	R_1 (%)	R_2 (%)	R_1 (%)	R_2 (%)	R_1 (%)	R_2 (%)
400	25.0	25.5	25.5	26.5	24.4	25.3	25.5	26.3
420	25.0	25.6	25.7	26.7	24.6	25.5	25.4	26.2
440	25.2	25.8	25.9	26.9	24.9	25.8	25.4	26.1
460	25.7	26.3	26.1	27.1	25.3	26.4	25.5	26.2
470	**25.9**	**26.5**	**26.4**	**27.3**	**25.6**	**26.6**	**25.7**	**26.4**
480	26.1	26.7	26.6	27.4	25.8	26.8	25.8	26.5
500	26.6	27.2	26.9	27.7	26.3	27.0	26.3	26.9
520	27.0	27.6	27.2	27.9	26.7	27.4	26.9	27.5
540	27.4	28.0	27.4	28.1	27.0	27.6	27.5	28.0
546	**27.5**	**28.1**	**27.5**	**28.2**	**27.1**	**27.7**	**27.7**	**28.2**
560	27.6	28.3	27.6	28.3	27.2	27.8	28.0	28.5
580	27.7	28.4	27.8	28.5	27.3	27.9	28.5	28.9
589	**27.8**	**28.4**	**27.9**	**28.6**	**27.4**	**28.0**	**28.7**	**29.1**
600	27.8	28.4	27.9	28.6	27.4	28.0	28.8	29.3
620	27.8	28.4	27.9	28.6	27.5	28.0	29.0	29.5
640	27.7	28.4	27.9	28.6	27.5	27.9	29.1	29.6
650	**27.7**	**28.4**	**27.9**	**28.6**	**27.5**	**27.9**	**29.2**	**29.6**
660	27.7	28.4	27.9	28.6	27.5	27.9	29.2	29.6
680	27.7	28.3	27.9	28.6	27.5	27.9	29.2	29.6
700	27.7	28.3	27.9	28.6	27.5	27.9	29.2	29.6

Note: The values required by the Commission on Ore Mineralogy are given in bold.

https://doi.org/10.1180/mgm.2023.78 Published online by Cambridge University Press

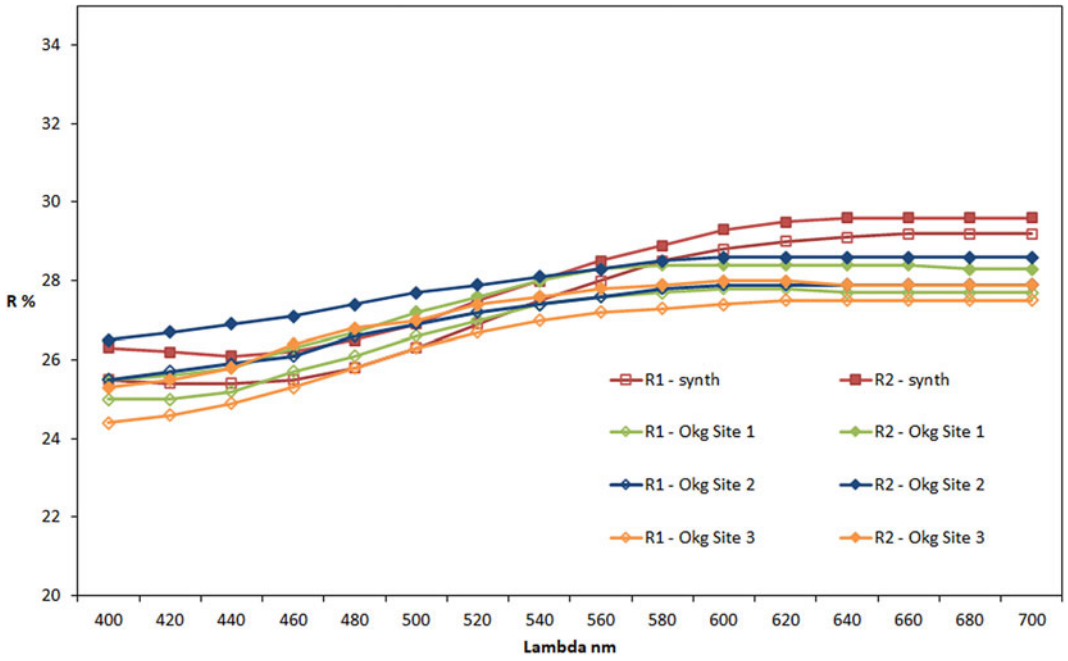

Figure 4. Reflectance data for okruginite, measured on 3 sites and its synthetic analogue. The reflectance values (*R*%) are plotted versus wavelength λ in nm.

on the Cu*L*α, Sn*L*α and Se*L*α (with an overlap correction on SnL_{c3}) lines with an accelerating voltage of 15 keV, and a beam current of 10 nA on the Faraday cup.

The results are given in Table 2. The empirical formula of okruginite calculated on the basis of 6 apfu is $Cu_{1.99}Sn_{1.02}(Se_{1.82}S_{1.17})_{\Sigma 2.99}$ and $Cu_{1.86}Sn_{1.03}Se_{3.11}$ for its synthetic analogue. Alternative recalculation of the empirical formula of okruginite based on 3 Se (Se+S) atoms yields $Cu_{1.99}Sn_{1.01}(Se_{1.83}S_{1.17})_{\Sigma 3.00}$ and $Cu_{1.79}Sn_{0.99}Se_{3.00}$ for its synthetic equivalent. The ideal formula Cu_2SnSe_3 requires Cu 26.33, Sn 24.59, Se 49.08, total 100 wt.%.

Synthetic analogue

The size (10–15 μm) of inclusions of okruginite, intimately intergrown with mohite or embedded in quartz, prevented their extraction in an amount required for relevant crystallographic and structural investigations. Therefore, these investigations were performed on the synthetic Cu_2SnSe_3.

The synthetic phase Cu_2SnSe_3 was prepared in an evacuated and sealed silica-glass tube in a horizontal furnace in the Laboratory of Experimental Mineralogy of the Czech Geological Survey in Prague. A charge of ~400 mg was carefully weighed out from the native elements. We used, as starting chemicals copper powder (99.9999% purity), tin ingot (99.9999% purity) and selenium pebbles (99.9999% purity). To prevent loss of material to the vapour phase during the experiment, the free space in the tube was reduced by placing a closely fitting silica glass rod against the charge. The evacuated tube with its charge was sealed and then annealed at 600°C for 1 week. After cooling by cold-water bath, the charge was ground into powder in acetone using an agate mortar, and thoroughly mixed to homogenise. The pulverised charge was sealed in an evacuated silica-glass tube again, and reheated at 200°C for 6 months. Afterwards, after homogenisation, the sample was heated at 500°C for 3 weeks and cooled in a slow regime (5°C per hour).

Table 2. Electron-microprobe analyses (wt.%) of studied grains of okruginite and its synthetic analogue.

		Cu	Sn	Se	S	Total
Okruginite	Ave.	29.48	28.10	33.40	8.75	99.73
(*n* = 27)	Max.	30.91	29.32	37.16	10.96	
	Min.	27.69	26.01	29.64	6.39	
	S.D.	0.96	0.81	2.38	1.41	
Synthetic Cu_2SnSe_3	Ave.	23.62	24.37	49.09		97.08
(*n* = 7)	Max.	23.71	25.45	49.28		
	Min.	23.54	23.82	48.84		
	S.D.	0.06	0.49	0.16		
Ideal composition		26.33	24.59	49.08		100.00

S.D. – Standard deviation

Table 3. Data collection and Rietveld analysis of synthetic of Cu_2SnSe_3, the synthetic analogue of okruginite.

Crystal data	
Space group	*Cc* (No. 9)
Unit-cell content	Cu_2SnSe_3, *Z* = 4
Unit-cell parameters (Å)	*a* = 6.9906(2)
	b = 12.0712(4)
	c = 6.9723(2)
	β =109.350(10)°
Unit-cell volume (Å^3)	555.1(2)
Data collection	
Radiation type, source	X-ray, Cu*K*α
Generator settings	40 kV, 30 mA
Range in 2θ (°)	10–140
Step size (°)	0.01
Rietveld analysis	
No. of reflections	535
No. of structural parameters	24
Isotropic crystal size (nm)	256(4)
R_{Bragg}	0.026
R_P	0.024
R_{wp}	0.034

https://doi.org/10.1180/mgm.2023.78 Published online by Cambridge University Press

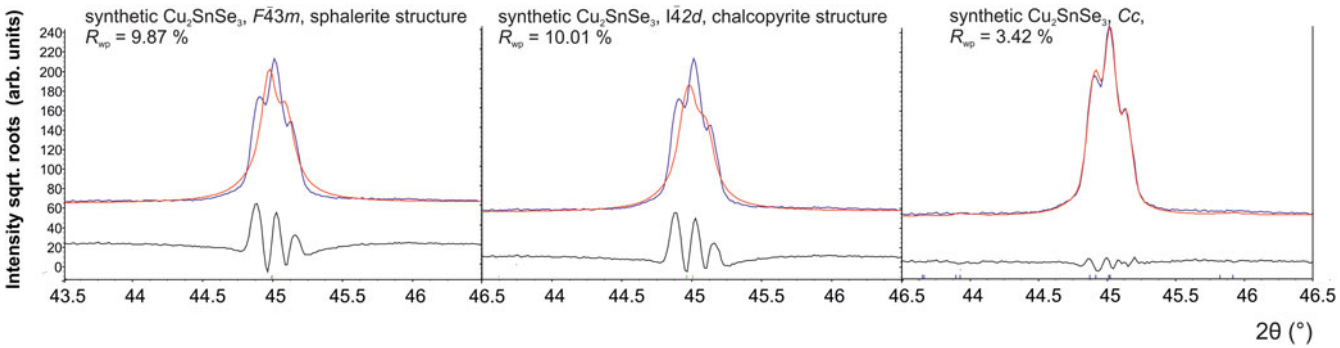

Figure 5. Detail of Rietveld fit of synthetic Cu_2SnSe_3, an analogue of okruginite, using sphalerite, chalcopyrite and *Cc* structure models. Only the model with *Cc* symmetry (Delgado *et al.*, 2003) can fit all the observed reflections in the diffraction pattern. Note the significant difference in the R_{wp} factor.

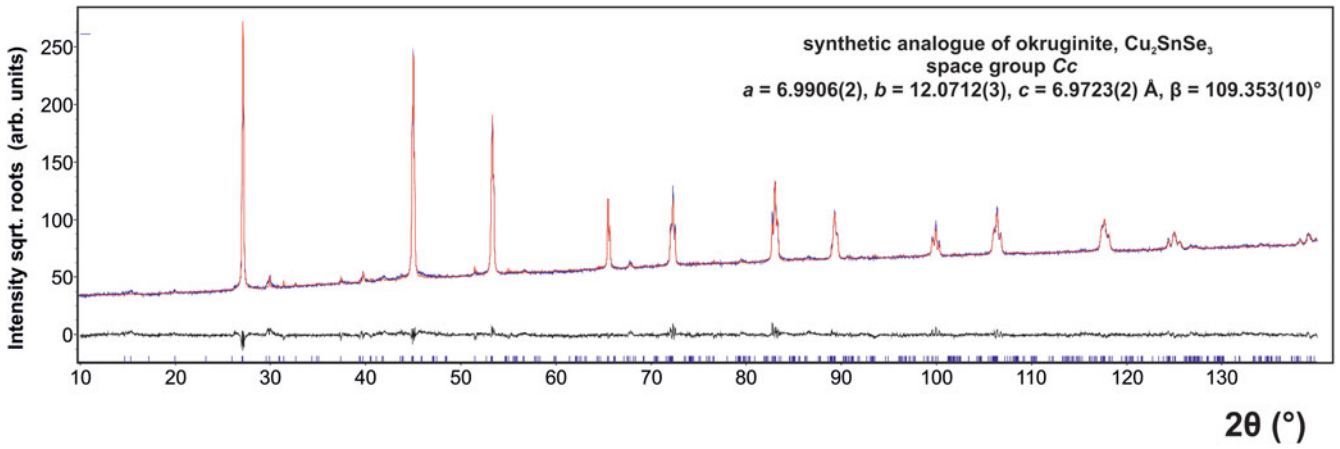

Figure 6. The final Rietveld fit for Cu_2SnSe_3, the synthetic analogue of okruginite.

X-ray crystallography

The powder X-ray diffraction pattern of synthetic Cu_2SnSe_3, used for structure refinement, was collected in Bragg-Brentano geometry on a Bruker D8 Advance diffractometer, equipped with a LynxEye XE detector using Cu*K*α radiation and a 10 mm automatic divergence slit. The data were collected in the angular range from 10 to 140° of 2θ with a 0.015° step and with a counting time of 1.4 sec per step. The details of data collection and basic crystallographic data are given in Table 3.

The crystal structure of Cu_2SnSe_3, the synthetic equivalent of okruginite was refined using the Rietveld method by the *Topas 5* program (Bruker AXS, 2014). Preliminary inspection of the powder data revealed that the main reflections can be indexed by a cubic sphalerite-based structure ($F\bar{4}3m$) with $a = 5.69$ Å, as was suggested by Sharma *et al.* (1977) for the synthetic Cu_2SnSe_3 phase. However, this cubic model could not fit weak superstructure diffractions visible in our powder X-ray diffraction pattern and could not describe visible peak splitting indicating lowering of the symmetry (Fig. 5). It is worth noting that even Sharma *et al.* (1977) observed peak splitting in the diffraction pattern of Cu_2SnSe_3 and mentioned that the true symmetry of the Cu_2SnSe_3 phase might be lower than the cubic one. All their attempts to index the collected Debye–Scherrer diffraction patterns of Cu_2SnSe_3 in lower symmetry cells failed. Based on the indexing of collected diffraction patterns, Hahn *et al.* (1966) proposed a tetragonal chalcopyrite-structure type ($I\bar{4}2d$ symmetry) for synthetic Cu_2SnSe_3. However, no proper crystal structure analysis (including the refinement of structure) was carried out in their original work; the atomic coordinates were taken from the Inorganic Crystal Structure Database (ICSD, 2023, #629091) and were estimated by an editor of the database. This tetragonal chalcopyrite-type structure model also does not account for observed peak splitting in the diffraction pattern. Subsequently, the monoclinic structure model (*Cc* symmetry) suggested by Delgado *et al.* (2003) and also later by Nomura *et al.* (2013) for the synthetic Cu_2SnSe_3 phase provides not only an accurate description of peak splitting, but also fits well to weak, though discernible, superstructure reflections (Fig. 6). The refinement of this monoclinic structure model resulted in a significant drop of R_{wp}

Table 4. Atomic positions (space group *Cc*) and isotropic displacement parameters for the synthetic analogue of okruginite, Cu_2SnSe_3. The isotropic displacement parameter (B_{iso}) was constrained for Cu/Sn and Se positions.

Atom	Wyckoff position	Occupancy	*x*	*y*	*z*	B_{iso} [Å^2]
Cu1/Sn1	4*a*	0.78/0.22(3)	0.376(3)	0.2555(7)	0.611(3)	0.5
Cu2/Sn2	4*a*	0.90/0.10(2)	0.379(2)	0.4164(15)	0.111(4)	0.5
Cu3/Sn3	4*a*	0.35/0.65(2)	0.373(2)	0.0871(11)	0.110(4)	0.5
Se1	4*a*	1	0.005(3)	0.4128(15)	−0.014(4)	0.8
Se2	4*a*	1	−0.016(3)	0.0845(16)	−0.013(4)	0.8
Se3	4*a*	1	0.503(2)	0.2590(15)	−0.014(2)	0.8

https://doi.org/10.1180/mgm.2023.78 Published online by Cambridge University Press

Table 5. Powder X-ray diffraction data (output from Rietveld refinement) of Cu_2SnSe_3, the synthetic analogue of okruginite (Cu$K\alpha$ radiation, Bruker D8 Advance, Bragg-Brentano geometry).

I_{calc}	I_{obs}	d_{calc}	*h k l*	I_{calc}	I_{obs}	d_{calc}	*h k l*
1	3	4.4474	0 2 1	6	3	1.1651	$\bar{6}$ 0 2
52	54	3.2978	2 0 0	12	6	1.1634	1 3 5
54	53	3.2892	0 0 2	10	6	1.1624	$\bar{3}$ 9 1
100	100	3.2864	$\bar{1}$ 3 1	11	6	1.1623	$\bar{4}$ 6 4
1	1	3.0178	0 4 0	6	4	1.1621	$\bar{2}$ 0 6
2	5	2.9887	$\bar{2}$ 2 1	10	6	1.1617	$\bar{1}$ 9 3
1	1	2.8497	1 3 1	2	1	1.0993	6 0 0
1	1	2.7430	0 4 1	4	3	1.0980	4 6 2
1	1	2.5757	$\bar{2}$ 2 2	3	1	1.0972	$\bar{6}$ 0 4
1	2	2.4038	2 2 1	5	3	1.0970	2 6 4
2	2	2.2671	1 5 0	4	2	1.0965	3 9 1
1	2	2.1629	3 1 0	2	1	1.0964	0 0 6
29	23	2.0183	2 0 2	0	0	1.0964	2 10 1
56	46	2.0164	$\bar{3}$ 3 1	4	2	1.0961	$\bar{5}$ 3 5
57	50	2.0125	$\bar{1}$ 3 3	4	2	1.0959	1 9 3
27	24	2.0119	0 6 0	3	2	1.0956	$\bar{4}$ 0 6
1	1	1.7746	1 5 2	5	3	1.0955	$\bar{3}$ 9 3
18	13	1.7211	3 3 1	1	1	1.0825	1 11 0
9	6	1.7200	$\bar{4}$ 0 2	4	2	1.0091	4 0 4
17	13	1.7187	1 3 3	7	4	1.0082	$\bar{6}$ 6 2
18	14	1.7175	2 6 0	7	4	1.0063	$\bar{2}$ 6 6
19	15	1.7171	$\bar{3}$ 3 3	3	2	1.0059	0 12 0
9	7	1.7163	$\bar{2}$ 0 4	3	2	0.9651	5 3 3
18	15	1.7163	0 6 2	3	2	0.9647	6 6 0
20	13	1.4249	2 6 2	0	0	0.9644	$\bar{7}$ 1 4
11	7	1.4240	$\bar{4}$ 0 4	3	2	0.9643	$\bar{7}$ 3 3
1	1	1.3818	$\bar{2}$ 8 1	3	2	0.9643	3 3 5
1	1	1.3305	$\bar{3}$ 5 4	3	2	0.9635	$\bar{5}$ 9 1
4	3	1.3103	4 0 2	4	2	0.9633	$\bar{6}$ 6 4
8	5	1.3095	$\bar{5}$ 3 1	3	2	0.9627	0 6 6
4	3	1.3087	2 0 4	4	2	0.9622	$\bar{4}$ 6 6
1	0	1.3076	2 8 1	3	2	0.9622	$\bar{3}$ 3 7
7	4	1.3073	$\bar{4}$ 6 2	3	2	0.9622	2 12 0
9	6	1.3062	$\bar{1}$ 3 5	3	2	0.9622	$\bar{1}$ 9 5
7	5	1.3057	$\bar{2}$ 6 4	3	2	0.9619	0 12 2
7	5	1.3055	$\bar{1}$ 9 1				
1	1	1.2430	0 8 3				
1	1	1.2427	$\bar{2}$ 8 3				
1	1	1.2074	$\bar{5}$ 5 2				
11	7	1.1657	5 3 1				

profile agreement factor from 9.87% ($F\bar{4}3m$ structure) to 3.42% (*Cc* structure).

The Rietveld refinement involved refinement of unit-cell parameters, background Chebychev polynomial of the 5th order, atomic coordinates, isotropic size and strain and occupancy parameters for Cu1, Cu2 and Sn positions. Our refinement revealed mixed sites at Cu1, Cu2 and Sn positions (see Table 4), indicating a partial Cu/Sn disorder at these positions. No mixed sites were revealed at Se positions.

No significant deviations of crystal coordinates from their starting positions (structure model of Delgado *et al.*, 2003) were observed; as the refined fractional coordinates do not deviate by more than 0.01 from the starting values. However, a partial disorder at Cu1, Cu2 and Sn positions was detected in our refinement (Table 4), which was not reported by Delgado *et al.* (2003). Crystal structure and powder diffraction data are presented in Tables 4 and 5, respectively. Okruginite shows monoclinic symmetry, however the mineral is strongly pseudocubic. Because of strong partial reflection overlapping in its powder diffraction pattern, it is not possible to fit individual positions and intensities of reflections and perform subsequent traditional unit-cell refinement based on d_{calc} and d_{obs}. Hence, output from Rietveld refinement is presented in Table 5 (only $I_{calc} \geq 1$ are presented). The final Rietveld fit is shown in Fig. 6. The crystallographic information files have been deposited with the Principal Editor of *Mineralogical Magazine* and are available as Supplementary material (see below).

Structure description

The okruginite crystal structure is shown in Fig. 7. It can be described as a derivative of the sphalerite structure. As is typical for this group of minerals, the cations (Cu1, Cu2 and Sn) show tetrahedral coordination by Se atoms. The tetrahedra share Se-corners and form a three-dimensional network. The Cu–Se distances are within the range 2.34–2.49 Å (mean value 2.43 Å),

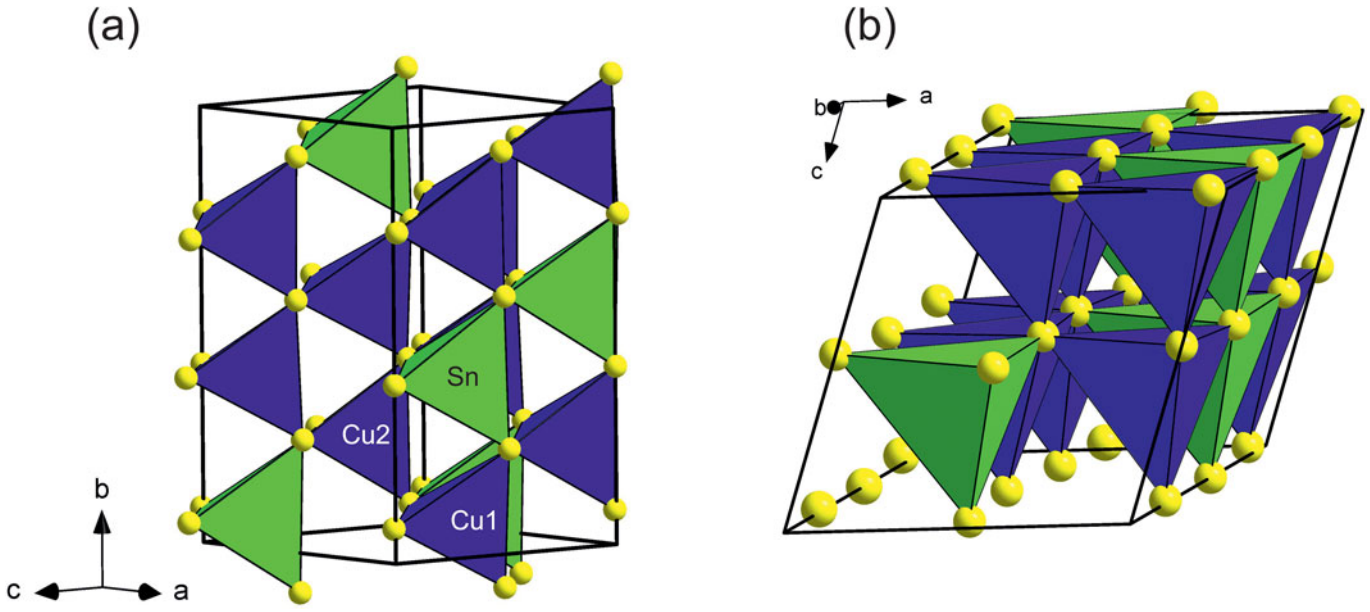

Figure 7. Crystal structure of Cu_2SnSe_3, the synthetic analogue of okruginite, showing tetrahedral coordination by selenium around Cu and Sn cations. Drawn using Diamond (Diamond - Crystal and Molecular Structure Visualization, Crystal Impact - Dr. H. Putz & Dr. K. Brandenburg GbR, Kreuzherrenstr. 102, 53227 Bonn, Germany, https://www.crystalimpact.de/diamond).

https://doi.org/10.1180/mgm.2023.78 Published online by Cambridge University Press

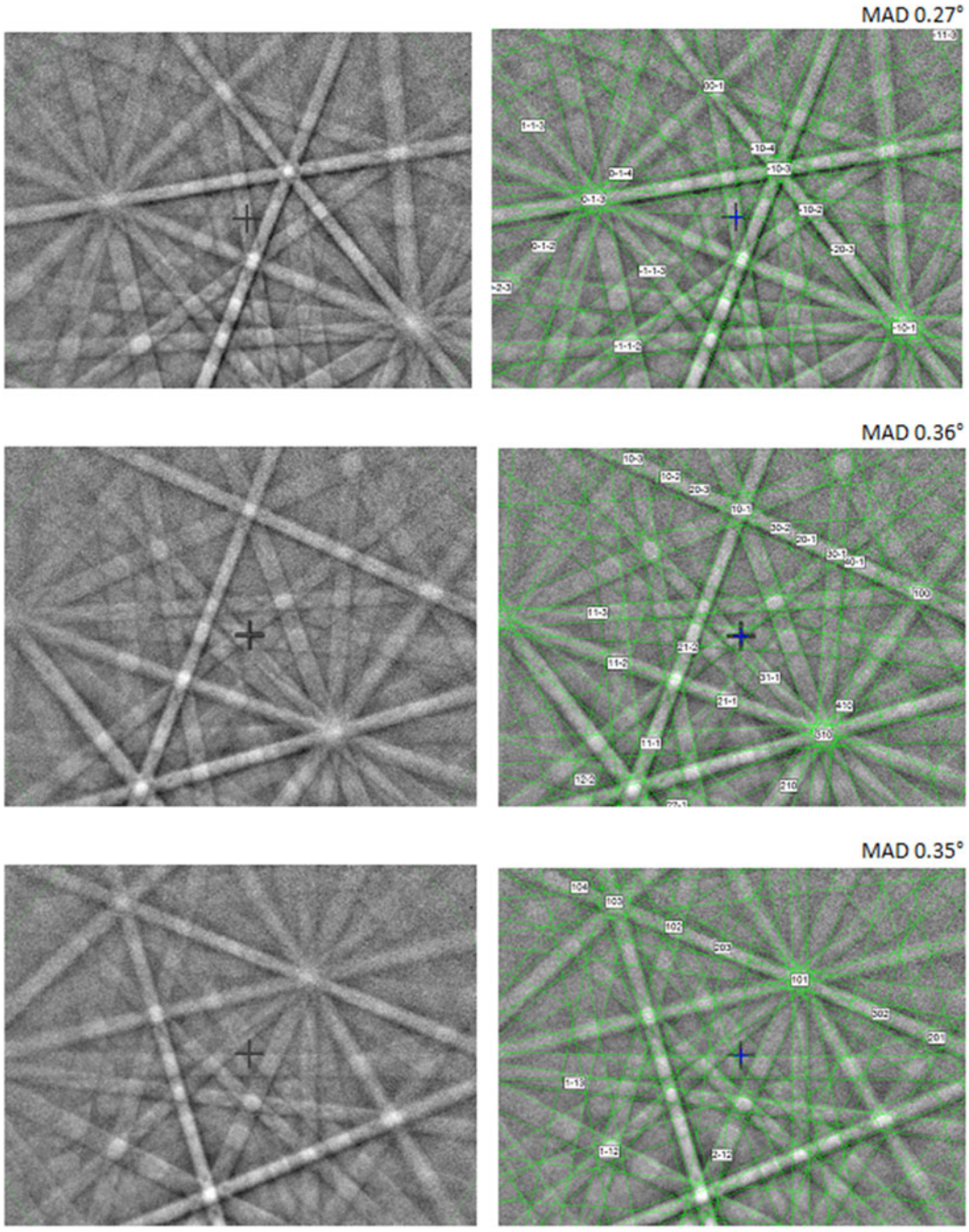

Figure 8. Electron back-scattered diffraction patterns from okruginite obtained from grains with different orientations; in the right pane the Kikuchi bands are solved (indexed). The cross marks the position of the pattern centre. Acquisition conditions were: accelerating voltage = 30 kV, beam current = 0.3 nA, no binning (full EBSD resolution is 1344 × 1024). Indexing conditions: 12 bands, 65 reflectors.

Sn–Se distances vary from 2.47 to 2.56 Å (mean value 2.53 Å). These mean values are comparable with bond distances observed in similar adamantine structures, e.g. eskebornite $CuFeSe_2$ (Cu–Se: 2.418–2.424 Å, Delgado *et al.*, 1992), synthetic phases $CuInSe_2$ (CuSe: 2.432 Å, Knight, 1992) and $Cu_2FeSnSe_4$ (Cu–Se: 2.417 Å, Sn–Se: 2.56 Å, Roque Infante *et al.*, 1997). From a chemical point of view, okruginite is a selenide analogue of mohite, Cu_2SnS_3. Mohite was described as a monoclinic mineral by Kovalenker *et al.* (1983), however its crystal structure has not been determined. A synthetic phase, Cu_2SnS_3 shows (at least three) modifications. The high-temperature modification (above 780°C) was reported by Palatnik *et al.* (1961) and by Moh (1963) with the sphalerite structure (i.e. disordered structure). Chen *et al.* (1998) described a tetragonal stannite-type structure for synthetic Cu_2SnS_3 prepared at 700°C. A monoclinic modification (*Cc* symmetry) was prepared by Onoda *et al.* (2000). Mohite is probably isostructural with this monoclinic modification of Cu_2SnS_3; however its direct detailed crystallographic study has not yet been performed. Okruginite is isostructural with this monoclinic Cu_2SnS_3 phase (Onoda *et al.*, 2000). Other chemically related minerals petříčekite $CuSe_2$ (Bindi *et al.* 2016) and svetlanaite SnSe (Okrugin *et al.*, 2022) adopt marcasite and GeS-type

https://doi.org/10.1180/mgm.2023.78 Published online by Cambridge University Press

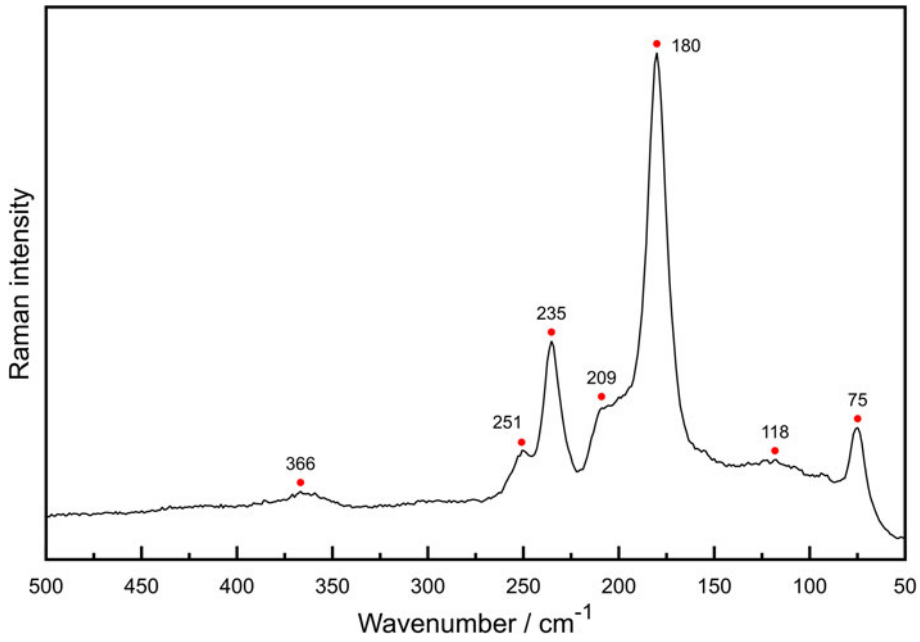

Figure 9. Raman spectrum of synthetic Cu_2SnSe_3 in the 50–500 cm^{-1} range.

structures, respectively, and hence are structurally very different from okruginite.

Our refinement of the synthetic analogue of okruginite revealed a partial disorder at the Cu1, Cu2 and Sn sites (i.e. Cu/Sn mixed sites) indicating that the structure is not fully ordered. By analogy to phase transitions observed for Cu_2SnS_3 phase, it is very likely that at higher temperatures (>600°C) okruginite transforms to a completely disordered sphalerite-based structure. The substitution of Se by S observed in natural material is in accordance with the work of Nomura *et al.* (2013), who described the Cu_2SnSe_3–Cu_2SnS_3 solid solution.

Proof of identity of natural and synthetic okruginite

The structural identity of natural okruginite and its synthetic analogue was supported by EBSD measurements on the natural sample and comparison of the structural model for Cu_2SnSe_3 from our Rietveld refinement. Rietveld refinement of synthetic Cu_2SnSe_3 confirmed the monoclinic structure model of Delgado *et al.* (2003), later also described by Nomura *et al.* (2013). Hence, this structural model for Cu_2SnSe_3 was used in the EBSD measurement of the natural material.

A TESCAN LYRA3 FEG SEM combined with an EBSD system (Oxford Instruments *AztecHKL* with NordlysNano EBSD detector) was used for the measurements. The sample surface was prepared for EBSD by polishing with colloidal silica followed by broad beam ion milling (Gatan PECS II argon ion beam system operated at 2 kV for 60 min). Acquisition conditions were: accelerating voltage = 30 kV, beam current = 0.3 nA and no binning (full EBSP resolution is 1344 × 1024). The measured EBSD patterns obtained from a natural sample (several measurements from different grains of okruginite with different crystallographic orientations) were compared with patterns generated from the cubic, tetragonal and monoclinic structural models described above. Indexing conditions were: refined accuracy mode, 12 bands, 65 reflectors (the monoclinic model). All three models gave an acceptable match with reasonable mean angular deviation (MAD, i.e. goodness of fit of the solution) ranging between 0.26° and 0.36° (Fig. 8). It should be noted that in general the positive match obtained with EBSD is not a conclusive proof of structural identity, as EBSD cannot necessarily distinguish between closely similar structures (i.e. different derivatives of the sphalerite structure) that differ in a few reflectors observable in specific orientations only. Nevertheless, our synthesis and the relatively recent works of Delgado *et al.* (2003) and Nomura *et al.* (2013) favour the monoclinic *Cc* structure for Cu_2SnSe_3. It is also very likely that the cubic and tetragonal modifications of Cu_2SnSe_3 exist at higher temperatures (i.e. above 600°C) and the monoclinic phase is stable at lower temperatures. Considering the paragenetic sequence (conditions of formation in Nature of ~200–300°C) of okruginite, this mineral shows very likely monoclinic structure with *Cc* symmetry observed for synthetic Cu_2SnSe_3 by this work. Furthermore, the optical properties of okruginite indicate the monoclinic symmetry.

Raman spectroscopy

The Raman spectroscopic investigation was carried out using a Renishaw inVia Reflex Raman system coupled with a Leica microscope. The samples were measured with a 100× objective lens with excitation provided by a 785 nm diode laser and the signal was recorded by a thermoelectrically cooled CCD detector (spectral range of 100–4000 cm^{-1}, spectral resolution of 2 cm^{-1}). To enhance the signal-to-noise ratio, 20 scans were accumulated, each 20 s exposure time, with laser power at the source kept at a maximum of 15 mW to avoid thermal degradation. A polystyrene standard was used to check the wavenumber calibration and the spectra obtained were analysed using the *GRAMS/AI 9.1* software package (Thermo Fisher Scientific).

We were able obtain the Raman spectrum of the synthetic phase which showed seven Raman bands around 75, 118, 209, 235, 251, and 366 cm^{-1} with the dominant band at 180 cm^{-1} (Fig. 9). These positions are generally in agreement with the Raman spectrum reported for monoclinic Cu_2SnSe_3 by Marcano *et al.* (2011) who also provided tentative band assignments. Based on this, the bands at 75, 180 and 251 cm^{-1} probably

https://doi.org/10.1180/mgm.2023.78 Published online by Cambridge University Press

represent A′ modes, and bands at 209 and 235 cm^{-1} A″ modes. The weak band around 366 cm^{-1} is probably an overtone of the strong 180 cm^{-1} band, but the other the weak band around 118 cm^{-1} has no counterpart in the spectra reported previously. We were unable to measure a Raman spectrum of the natural phase due to very small size of grains and spectral interferences from other phases (a S-rich analogue or Ti-oxides).

Acknowledgements. The authors acknowledge Ritsuro Miyawaki, Chairman of the CNMNC and its members for helpful comments on the submitted data. The comments made by Igor Pekov, an anonymous reviewer, and the Principal Editor Stuart Mills are greatly appreciated. This work was supported by the Grant Agency of Czech Republic (22-26485S). FK acknowledges support by the Center for Geosphere Dynamics (UNCE/SCI/00). VK acknowledges Tescan Ltd. for the opportunity to use Tescan SEMs and Oxford Instruments analytical equipment in their demo laboratory in Moscow.

Supplementary material. The supplementary material for this article can be found at https://doi.org/10.1180/mgm.2023.78.

Competing interests. The authors declare none.

References

Bindi L., Förster H.J., Grundmann G., Keutsch F.N. and Stanley C.J. (2016) Petříčekite $CuSe_2$, a new member of the marcasite group from the Předbořice Deposit, Central Bohemia Region, Czech Republic. *Minerals*, **6**, 33.

Bruker AXS (2014) *Topas 5, Computing Program*. Bruker AXS Gmbh, Karlrsuhe, Germany.

Chen X., Wada H., Sato A. and Mieno M. (1998) Synthesis, electrical conductivity, and crystal structure of $Cu_4Sn_7S_{16}$ and structure refinement of Cu_2SnS_3. *Journal of Solid State Chemistry*, **139**, 144–151.

Delgado J.M., Diaz de Delgado G., Quintero M. and Woolley J.C. (1992) The crystal structure of copper iron selenide, $CuFeSe_2$. *Materials Research Bulletin*, **27**, 367–373.

Delgado G.E., Mora A.J., Marcano G. and Rincón C. (2003) Crystal structure refinement of the semiconducting compound Cu_2SnSe_3 from X-ray powder diffraction data. *Material Research Bulletin*, **38**, 1949–1955.

Demin A.G. (2015) Ozernovskoye field as a new promising ore object of Central Kamchatka with complex ores for gold, tungsten, silver and copper. *Zoloto i tekhnologii*, **1**(27), 12 [In Russian]

Hahn H., Klingen W., Ness P. and Schulze H. (1966) Ternaere Chalkogenide mit Silicium, Germanium und Zinn. *Naturwissenschaften*, **53**, 18.

ICSD (2023) *Inorganic Crystal Structure Database*. FIZ Karlsruhe – Leibniz-Institut für Informationsinfrastruktur, Karlsruhe, Germany.

Roque Infante E., Delgado J.M. and Lopez Rivera S.A. (1997) Synthesis and crystal structure of $Cu_2FeSnSe_4$, a (I2 II IV VI4) semiconductor. *Materials Letters*, **33**, 67–70.

Knight K.S. (1992) The crystal structures of $CuInSe_2$ and $CuInTe_2$. *Materials Research Bulletin*, **27**, 161–167.

Kovalenker V.A. (1983) Mohite, Cu_2SnS_3, a new sulfide of tin and copper. *International Geology Review*, **25**, 117–120. [in Russian]

Kovalenker V.A. and Plotinskaya O.Y. (2005) Te and Se mineralogy of Ozernovskoe and Prasolovskoe epithermal gold deposits, Kuril–Kamchatka volcanic belt. *Geochemistry, Mineralogy and Petrology* (*Sofia*), **43**, 118–124.

Litvinov A.F., Patoka M.G. and Markovsky B.A. (editors) (1999) *Map of mineral resources of Kamchatka region, explanatory memorandum and legend*. 1 map on 18 sheets, scale 1:500,000. Ministry of Natural Resources of the Russian Federation, Natural Resources Committee of Kamchatka Region and Koryak Autonomous Area, VSEGEI. St Petersburg, Russia.

Marcano G., Rincón C., López S.A., Pérez G.S., Herrera-Perez J.L., Mendoza-Alvarez J.G. and Rodríguez P. (2011) Raman spectrum of monoclinic semiconductor. *Solid State Communications*, **151**, 84–86.

Moh G. (1963) Sulphide systems containing Sn. *Carnegie Institute Yearbook*, **62**, 197.

Nomura T., Maeda T., Takei K., Morihama M. and Wada T. (2013) Crystal structures and band-gap energies of $Cu_2Sn(S,Se)_3$ ($0 \leq x \leq 1.0$) solid solution. *Physica status solidi*, **10**, 1093–1097.

Okrugin V.M., Vymazalová A., Kozlov V.V., Laufek F., Stanley C.J. and Shkilev I.A. (2022) Svetlanaite, SnSe, a new mineral from the Ozernovskoe deposit, Kamchatka peninsula, Russia. *Mineralogical Magazine*, **86**, 234–242.

Onoda M., Chen X.A., Sato A. and Wada H. (2000) Crystal structure and twinning of monoclinic Cu_2SnS_3. *Materials Research Bulletin*, **35**, 1563–1570.

Palatnik L.S., Komnik Yu.F., Belova E.K. and Adroschenko L.V. (1961) A group of semiconducting compounds containing Cu and elements from groups IV and VI. *Doklady Akademii Nauk SSSR*, **137**, 68–71.

Pekov I.V., Britvin S.N., Pletnev P.A., Chukanov N.V., Belakovskiy D.I. and Yapaskurt V.O. (2021) Ozernovskite, IMA 2021-059. CNMNC Newsletter 63. *Mineralogical Magazine*, **85**, https://doi.org.10.1180/mgm.2021.74

Pekov I.V., Britvin S.N., Pletnev P.A., Yapaskurt V.O., Belakovskiy D.I., Chukanov N.V., Vigasina M.F. and Ponomarev A.P. (2022) Rudolfhermannite, IMA 2021-099. CNMNC Newsletter 66. *Mineralogical Magazine*, 86, https://doi.org/10.1180/mgm.2022.33

Petrenko I.D. (1999) *Gold-silver formation of Kamchatka*. St. Petersburg, VSEGEI, 115 pp. [in Russian]

Sharma B.B, Ayyar R. and Singh H. (1977) Stability of the tetrahedral phase in the $A^I_2B^{IV}C^{VI}_3$ group of compounds**.** *Physica Status Solidi*, **40**, 691–696.

Spiridonov E.M., Ivanova Yu.N. and Yapaskurt V.O. (2014) Selenide goldfieldite and solid solutions of fischesserite $AuAg_3Se$ - petzite $AuAg_3Te$ in ores of the volcanogenic gold Ozernovskoe deposit (Kamchatka). *Doklady Earth Sciences*, **458**, 209–221 [in Russian].

Spiridonov E.M., Ignatov A.I. and Shubina E.V. (1990) The evolution of fahlores from the Ozernovskoe volcanogenic deposit (Kamchatka). *Izvestia Academy of Sciences USSR, Geology series*, **9**, 82–94 [in Russian].

Spiridonov E.M., Filimonov S.V. and Bryzgalov I.A. (2009) Solid solutions of fischesserite – naumannite $(Ag,Au)_2Se$ in ores of the volcanogenic gold Ozernovskoe deposit (Kamchatka). *Doklady Earth Sciences*, **425**, 391–394 [in Russian]

Strunz H. and Nickel E.H. (2001) *Strunz Mineralogical Tables, Ninth Edition*. Schweizerbart'sche Verlagsbuchhandlung, Stuttgart, Germany, 870 pp.

Vymazalová A., Kozlov V.V., Laufek F., Stanley C.J. and Shkilev I.A. (2023) Okruginite, IMA 2022-096. CNMNC Newsletter No. 71. *Mineralogical Magazine*, **87**, https://doi.org/10.1180/mgm.2023.11.